Benefit of higher closed–loop bandwidths in ocular adaptive optics

Luis Diaz-Santana, Cristiano Torti

Applied Vision Research Centre, Department of Optometry and Visual Science, City University, Northampton Square, London EC1V 0HB, UK

L.Diaz-Santana@city.ac.uk

Ian Munro, Paul Gasson

Photonics Group, Blackett Laboratory, Imperial College London, Prince Consort Road, London SW7 2BW UK

Chris Dainty

Applied Optics, Department of Experimental Physics, National University of Ireland, University Road, Galway, Ireland

Abstract: We present an ocular adaptive optics system with a wavefront sampling rate of 240 Hz and maximum recorded closed-loop bandwidth close to 25 Hz, but with typical performances around 10 Hz. The measured bandwidth depended on the specific system configuration and the particular subject tested. An analysis of the system performance as a function of achieved bandwidth showed consistently higher Strehl ratios for higher closed-loop bandwidths. This may be attributed to a combination of limitations on the available technology and the dynamics of ocular aberrations. We observed dynamic behaviour with a maximum frequency content around 30 Hz.

OCIS codes: (010.1080) Adaptive optics; (330.5370) Physiological optics; (330.4460) Ophthalmic optics

References and links

1. M.S. Smirnov, "Measurement of the wave aberration of the human eye," Biophys. **7**, 766–795 (1961).
2. J. Liang and D.R. Williams, "Supernormal vision and high resolution retinal imaging through adaptive optics," J. Opt. Soc. Am. A. **14**, 2884–2892 (1997).
3. R. Navarro, E. Moreno-Barriuso, S. Bara, and T. Mancebo, "Phase plates for wave-aberration compensation in the human eye," Opt. Lett. **25**, 236–238 (2000).
4. H. Hofer, L. Chen, G.Y. Yoon, B. Singer, Y. Yamauchi, and D. R. Williams, "Improvement in retinal image quality with dynamic correction of the eye's aberrations," Opt. Express **8**, 631–643 (2001), http://www.opticsexpress.org/abstract.cfm?URI=OPEX-8-11-631.
5. E.J. Fernández, I. Iglesias, and P. Artal. "Closed-loop adaptive optics in the human eye," Opt. Lett. **26**, 746–748 (2001).
6. M. Glanc, "Applications ophtalmologiques de l'optique adaptive," PhD thesis, Université de Pais-Sud (2002).
7. A. Roorda, F. Romero-Borja, W.J. Donnelly III, H. Queener, T.J. Hebert, and M.C.W. Campbell, "Adaptive optics scanning laser ophthalmoscopy," Opt. Express **10** 405–412 (2002), http://www.opticsexpress.org/abstract.cfm?URI=OPEX-10-9-405.
8. N. Doble, G. Yoon, L. Chen, P. Bierden, B. Singer, S. Olivier, and D.R. Williams, "Use of a michroelectromechanical mirror for adaptive optics in the human eye," Opt. Lett. **27**, 1537–1539 (2002).
9. H. Hofer, P.Artal, B.Singer, J.L. Aragón, and D.R. Williams, "Dynamics of the eye's wave aberration," J. Opt. Soc. Am. A **18**, 597–506 (2001).
10. L. Diaz Santana Haro and J.C. Dainty, "Effects of retinal scattering in the ocular double–pass process," J. Opt. Soc. Am. **18**, 1437–1444 (2001).

#2904 - $15.00 US Received August 15, 2003; Revised September 29, 2003

11. L. Diaz Santana Haro and J.C. Dainty, "Single–pass measurements of the wave-front aberrations of the human eye by use of retinal lipofuscin autofluorescence," Opt. Lett. **24**, 61–63 (1999).
12. A.V. Larichev, P.V. Ivanov, I.G. Iroshnikov, and V.I. Shmal'gauzen, "Measurement of eye aberrations in a speckle field," Quantum Electron. **31**, 1108–1112 (2001).
13. C. Paterson, I. Munro, and J.C. Dainty, "A low cost adaptive optics system using a membrane mirror," Opt. Express **6**, 175–185 (2000), http://www.opticsexpress.org/abstract.cfm?URI=OPEX-6-9-175.
14. H.T. Kasprzak and J.W. Jaronski, "Measurement of fine dynamic changes of the corneal topography by use of interferometry," in Interferometry XI: Applications, Proc. SPIE, **4778**, 169–176 (2002).

1. Introduction

Ocular aberrations limit the optical performance of the eye. In 1961 Smirnov [1] proposed to improve this performance by correcting ocular aberrations; however it was not until 1997 that Liang and Williams [2] achieved this, in a static fashion, for the first time with the help of adaptive optics technology. Since then, high costs, technical difficulties, and technological limitations have made progress in this area very slow. Static correction was again reported in 2000 with a completely different approach by Navarro *et al.* using phase plates [3] instead of a deformable mirror. It was not until 2001 (four years after Liang and Williams' work) that dynamic correction of ocular aberrations was reported by Hofer *et al.* [4] and by Fernández *et al.* [5], both reporting system bandwidths of approximately 2 to 5Hz, and more recently by Glanc [6]. In 2002, Roorda *et al.* [7] built an open loop confocal scanning laser ophthalmoscope that incorporated adaptive optics to achieve higher resolution images of the retina. That same year, the team of Williams reported a lower cost adaptive optics system with a similar bandwidth [8]. However, the closed-loop bandwidth of all these systems has stayed below approximately 5 Hz.

Hofer *et al.* [9] reported that according to their calculations "a perfect adaptive optics system with a closed-loop bandwidth of 1–2 Hz could correct these aberrations well enough to achieve diffraction-limited imaging over a dilated pupil." In this paper we show that a non–perfect (real) adaptive optics system can benefit from larger bandwidths. We present an adaptive optics system incorporating two novel features. Firstly, the framing rate of the system is 240 Hz allowing a typical closed loop bandwidth of approximately 10 to 12 Hz, but with performance as high as 25 Hz. Secondly, it uses, for the first time apart from a scanning laser ophthalmoscope design, a scanned beam in the wavefront sensing channel to eliminate speckle and to improve the signal to noise ratio of the Shack-Hartmann spots. This idea was originally proposed by Hofer *et al.* for ocular wavefront sensing [9], but it has never before been implemented for closed loop operation of an adaptive optics system. With this high frame rate, ocular speckle is an important problem with a large impact on the stability of the control servo-loop. The introduction of the scanner allowed the system to be more stable.

A systematic study of the system's performance and closed loop bandwidth was also carried out. The results show that the performance of the system is improved as the closed-loop bandwidth is increased. They also show, in agreement with previous work, that most of the aberration power is concentrated in the low frequencies, whilst the higher frequencies produce a much smaller degradation of image quality. However, our results show that with the currently available technology, higher bandwidths may be a cost effective approach for optimising ocular adaptive optics. This conclusion is in contrast with the general feeling that a closed loop correction of 5 Hz is sufficient for optimal high resolution retinal imaging with the technology currently available for wavefront correction.

2. Experimental setup

Figure 1 shows a schematic diagram of the optical layout. The system uses a Shack–Hartmann (SH) wavefront sensor consisting of an array of 0.2 mm square lenslets of focal length 25 mm

#2904 - $15.00 US Received August 15, 2003; Revised September 29, 2003

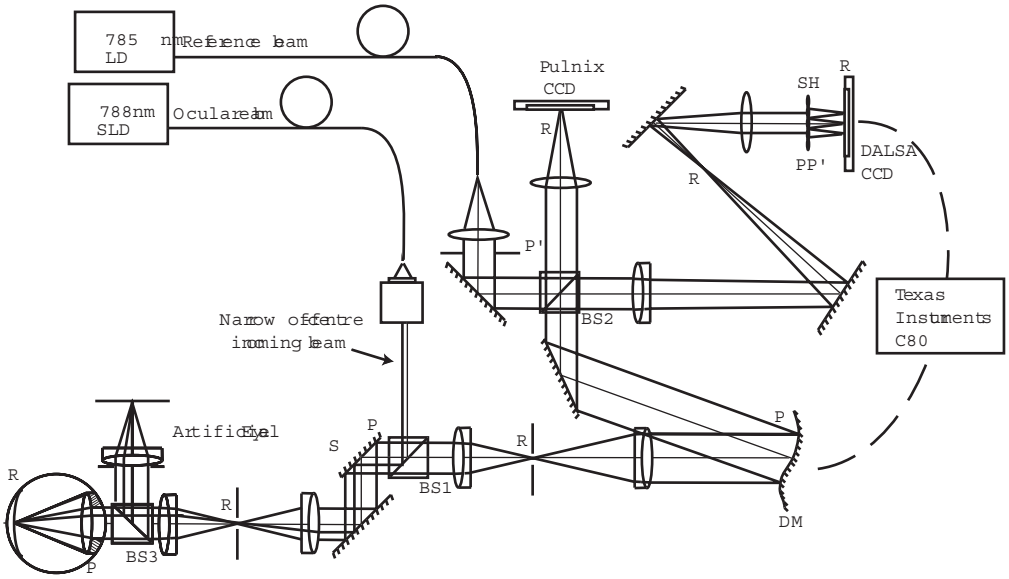

Fig. 1. Schematic diagram of the optical setup.

(LA) and a high speed CCD (DALSA CA-D1-0128A) with 128×128, 16μm square pixels, which has a maximum frame rate of about 780 Hz. The amount of light reflected from the retina is limited by ensuring that a safe level of light is put into the eye. This, combined with our technical ability to drive the CCD camera at a fixed set of frame rates restricted the camera to operating at approximately 240 Hz. The correcting element is an electrostatic membrane mirror (DM) supplied by OKO Technologies. It has a membrane of diameter 15 mm with 37 closed-pack hexagonal electrodes of spacing 1.75 mm. The light source used is a fiber coupled super luminescent diode (SLD) centered at 788 nm with an approximately 20 nm bandwidth. The use of an SLD reduces the amount of speckle in the wavefront signal. However, due to the high frame rate utilized, speckle is still a major source of noise [10, 11, 12]; hence the need for a scanner (S). The expanding beam from the single mode fiber is collimated using a microscope objective producing an approximately 2 mm diameter beam sent into the eye. System and corneal reflections are eliminated using the method proposed by Diaz-Santana and Dainty [11] and later improved by Hofer *et al.* [9] using an off axis beam. The scanner (S) is in a plane conjugated with the front nodal point of the eye, hence ensuring that the beam is de-scanned on the way out. The maximum angle of scanning is approximately one minute of arc.

The correcting mirror and the wavefront sensor all lie in planes conjugate to the eye pupil (P) whereas the retina (R) is conjugated with the CCD detectors. The eye pupil is magnified 1.6 times in the membrane mirror plane. The effective diameter of the mirror used was only 6.2 mm, corresponding to approximately 4 mm of the eye pupil. The pupil image is then demagnified 3.84 times in the wavefront sensor plane. A total of 21 lenslets were used for wavefront sensing. To maximise the amount of light reaching the wavefront sensor, the beamsplitter BS1 has a 30/70 reflection/transmission (R/T) ratio and the beamsplitter BS2 has a 80/20 R/T ratio. A $\times$40 microscope objective is used to magnify the image of the double-pass PSF into a Pulnix CCD camera PE2015 NIR connected to a video recorder to monitor the system's performance

#2904 - $15.00 US
Received August 15, 2003; Revised September 29, 2003

(note that only the second–pass PSF is being corrected). A reference arm provides a collimated beam used to calibrate the wavefront sensor. The light source for this arm is a fiber coupled laser diode (LD) centered at 785 nm. The exit pupil of the collimator (P′) is conjugated with the lenslet array.

The system control is performed using a single Texas Instruments C80 digital signal processor board housed in a standard desktop PC. The system was controlled using modified software based on that described by Paterson *et al.* [13] and identical hardware. The temporal control system is a simple integrator with a user controllable gain. This can be used to control the bandwidth of the system. The processing delay depends on the setup, but typically the correction is calculated and applied before 10% of the following image has arrived from the framegrabber. However, the delay between the arrival of light at the wavefront sensor and the transfer to the computer is harder to determine. It was estimated from looking at the first few frames of the sensor data where the system "sees" its own response within a maximum of two frames of starting to apply the correction. The system incorporates a simple artificial eye through a removable beam-splitter (BS3) consisting of a scattering "retina" and a lens doublet. This is used both to calibrate the system and to provide a static subject for comparison with real eyes. The calibration consisted of applying a voltage to each electrode sequentially, and recording the resulting effect on the wavefront sensor signals thereby establishing an actuator-sensor interaction matrix for the system [13]. This process creates a basis of functions that can be used to describe a wavefront and that match the geometry of the correcting mirror. Each one of these functions is called a "mode".

3. Experimental protocol

The system was tested with seven subjects aged 22 to 30 years old. Five of them with 6/6 visual acuity or better without spectacle correction. Two of them had visual acuity below 6/7.5 without correction. One of them achieved 6/5-1 after correcting sphere (-1.25D), whilst the other one achieved 6/6 -1 with her contact lenses on the tested eye. These two subjects were tested in the AO system wearing this correction; all other subjects did not wear spectacle correction. All subjects were tested under normal conditions of accommodation in a dark room to allow natural pupil dilation. The correction was achieved over a pupil of approximately 4mm diameter. All subjects fixated on the line formed by the scanner over the retina, which was at infinity.

The system was first tested with four of these subjects. This testing consisted of video recording the double–pass PSF of the tested eye with and without adaptive compensation. A systematic study of the system performance was then carried out. Four subjects were involved in this study. Only one subject participated in both parts of the experiment.

The data acquisition protocol was the following. Before the first correction attempt, the mirror was pre-biased, the positions of the SH spots from the reference beam were saved and the singular value decomposition of the control matrix was computed, from an average of five calibration steps, using the artificial eye. Once the number of modes to correct had been chosen, the subject's eye was aligned with the system. For this, the subject's head was stabilised using a "bite bar". Alignment was achieved by overlapping the SH spots from the eye with those from the reference arm while the subject fixated on the spot of light formed on the retina by the incoming beam (perceived as a horizontal line due to scanning). The subject was asked to remain still while the system was in adaptive mode. The calculated displacements of the SH spots from the reference position were recorded for 1000 iterations (approximately 4 s at 240 Hz for later reconstruction of the wavefront) immediately after engaging adaptive correction.

Once the first correction attempt was performed, there was no need to re-save the reference spots positions. In the cases of a parameter change, the system was re-calibrated; but realignment of the eye with the system was repeated every time a new set of data was taken. The total

#2904 - $15.00 US Received August 15, 2003; Revised September 29, 2003

power into the eye in all cases was less than 40 μW. Informed consent was requested from all subjects prior to the experiment.

For the first part of this study the system gain and the number of modes to be corrected were kept fixed at 0.2 and 14 respectively, for all data sets recorded. Here, gain refers to the feedback control parameter that quantifies the contribution that the feedback signal from the *i*th iteration of wavefront measurement makes to the (i+1)th iteration of wavefront control. The double–pass PSF imaged on the Pulnix CCD camera was recorded in video format for comparison with the recorded signals from the wavefront sensor. This information was fundamental for relying solely on the signals from the wavefront sensor as an approximate metric of performance.

The second part of this study consisted of longer experimental sessions in which the system gain and the number of corrected modes were systematically varied in order to gain an understanding of the optimal configuration of the system and their impact on wavefront correction. Due to time restrictions and the slowness of the procedure, the optimal number of modes to correct was first found for each subject with a gain of 0.2 and then the system's gain was systematically varied, keeping fixed the optimal number of corrected modes. The optimal number of modes to correct was defined as the maximum number of corrected modes that clipped a minimum number of mirror driving voltages. This metric of performance does not necessarily provide the best possible Strehl ratio. This procedure was chosen due to the time constrains involved: estimating the Strehl ratio for every run was very time consuming and not at all practical during the experimental session. For each configuration (gain and number of corrected modes), a minimum of three data sets were recorded. Additionally, a minimum of two data sets were recorded without adaptive compensation. The double-pass PSF was not analysed due to the time restrictions involved on the session and the larger times required for digitally analysing video files. However, based on the results from the first part of the study, the system performance was estimated from the wavefront sensor signals.

4. Data analysis

For the first part of the study the video recorded double–pass PSF were compared with the deviation of the recorded wavefront signals from their off-set positions. Unfortunately, a quantitative comparison was difficult due to noise and interlacing introduced in the video format. A Wiener deconvolution was attempted to extract the single-pass information from the double-pass PSF, but again noise issues prevented us from successfully completing this task. Nevertheless, in all cases a qualitative agreement between the narrowing of the double-pass PSF with adaptive compensation and a reduction in the displacements of the SH spots from their zero position (before and after correction) was observed. This was a fast and reliable method for gaining insight into the performance of the system without having to reconstruct the ocular wavefront and its rms value during the experimental session.

Once it had been confirmed that the wavefront sensor signals corresponded well with the observed results, the performance of the system was evaluated directly from the wavefront sensor signals. Note however, that the results obtained in this way may have shown lower wavefront errors (that is, better Strehl ratios) than those actually produced by the system.

For the second part of the study, the data was analysed as follows: From the wavefront sensor signals from 1000 recorded frames the corresponding ocular wavefronts were estimated. The wavefront rms and Strehl ratios were then estimated. The power spectra of the wavefront rms were then calculated for every one of the last 975 recorded frames. The bandwidth achieved for that particular run was estimated by comparing the calculated power spectrum, with correction, with the power spectrum of the same eye without correction. The first 25 rms values were not used to calculate the power spectra to eliminate the initial peak (drop of the wavefront rms) produced when engaging adaptive correction.

#2904 - $15.00 US Received August 15, 2003; Revised September 29, 2003

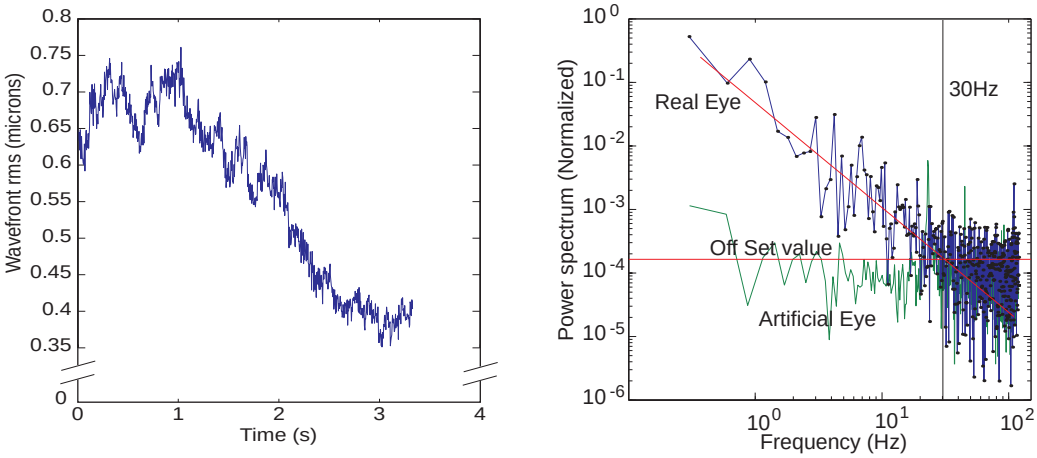

Fig. 2. Dynamics of ocular aberrations. (a) Wavefront rms measured at 240 Hz over approximately 4 s. (b) Power spectrum of the signal in (a) showing dynamic behaviour in excess of 30 Hz.

The Strehl ratio for each run was also estimated from the wavefront sensor signals. Its mean value and standard deviation over the same 975 frames used to estimate the power spectra were calculated. Finally, the closed–loop bandwidths were compared against the Strehl ratios and plotted to investigate any trends.

5. Results

Ocular aberrations without adaptive compensation were recorded for four subjects over four seconds. The power spectrum of the signal was calculated to analyse its frequency content. This analysis revealed temporal frequencies close to 30 Hz in three out of four subjects. The Shack-Hartmann spots from the fourth subject had a very low signal–to–noise ratio giving a very high offset value that only allowed visualisation of dynamic behaviour under 15 Hz.

Figure 2(a) shows the wavefront rms over 800 frames (3.3 s) without adaptive compensation for subject JK. This particular wavefront signal clearly shows a large and slow change in the wavefront rms (from 0.7 to 0.5μm) over two seconds. Superimposed on this are faster changes in the rms value. This behaviour was observed in all eyes, and is better described by the power spectrum of the wavefront rms signal. Fig. 2(b) shows this from Fig. 2(a). The off-set value was calculated as the mean of the artificial eye's power spectrum. The fit to the signal is a least squares fit to the logarithm of the power spectrum against the logarithm of the frequencies. All subjects showed a similar power spectrum fitting a straight line in a log–log plot with slope close to 1.5. This particular example exhibits frequency content up to 30 Hz.

The system successfully reduced the ocular wavefront aberration in all seven subjects tested

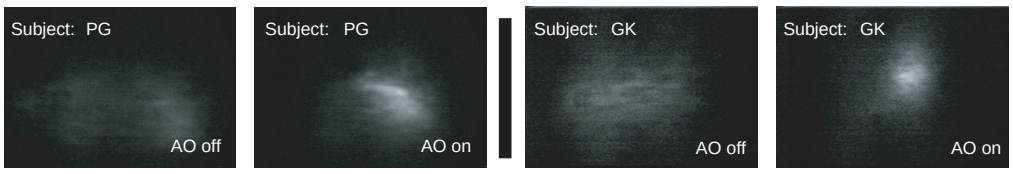

Fig. 3. Asymmetric ocular double–pass PSF with and without adaptive compensation.

#2904 - $15.00 US
Received August 15, 2003; Revised September 29, 2003

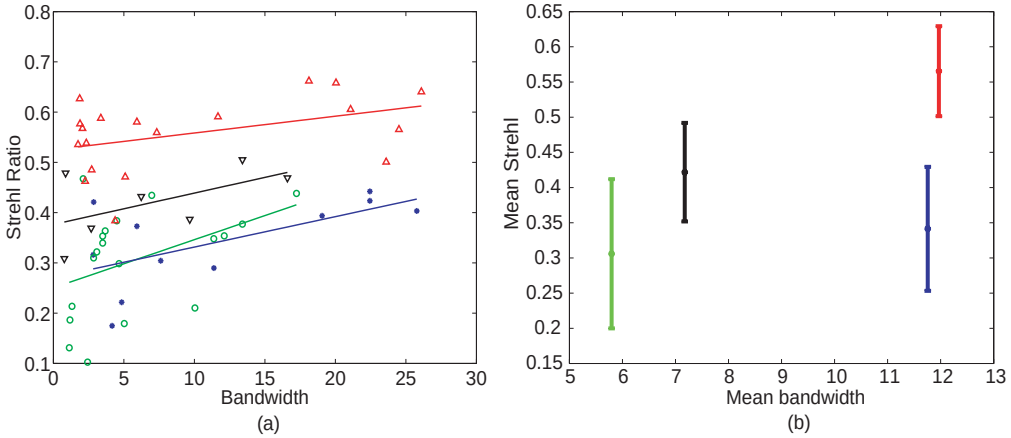

Fig. 4. System's performance as a function of bandwidth

(JB GK PG LD CT JK CG). This was evident as a narrowing of the double–pass PSF in all subjects tested when the adaptive correction was activated. Figure 3 shows two examples of this: the recorded double-pass PSF before, (left panels) and after correction (right panels) for subjects PG and GK.

Closed–loop bandwidths were estimated for every recorded run by finding the cross-over between the corrected and non-corrected power spectra. This was achieved using a least square fit to each signal. The observed closed-loop bandwidth for each run was very variable, even when keeping all system parameters fixed between two separate runs. Nevertheless, it was possible to exert some control over the closed-loop bandwidth by varying the gain of the system's control servo-loop. Servo-loop gains of 50% to 60% produced the best system performance for all four subjects.

Figure 4(a) shows the performance of the system as a function of the bandwidth achieved. The horizontal axis is the system's bandwidth while the vertical axis is the mean of the Strehl ratio (estimated form the wavefront sensor signals) achieved. The mean value plotted was calculated as described in Section 4. The straight lines are the least square fit for each subject. All of them show a positive slope, indicating a better performance for higher bandwidths. Table 1 shows the correlation coefficients estimated from the data and the corresponding p values. These results show that the observed improvement in system's performance could be attributed with at least 90% confidence to the increased closed-loop bandwidth in three out of four subjects.

Figure 4(b) shows the mean values for each subject in Fig. 4(a). This shows again a trend for improved Strehl ratios with higher bandwidths.

6. Discussion

Adaptive optics for high resolution retinal imaging poses many challenges: most of the techniques and technology used originate from astronomical adaptive optics. In astronomy, costs are usually not an issue, and adaptive optics systems for telescopes are custom designed for a particular site and instrument. Adaptive optics for the eye, by contrast, is limited by budgetary constraints and needs to make best use of the available (usually low cost) technology. Moreover, there is little information about issues such as noise, speckle, error propagation and the dynamics of ocular aberrations. Optimisation of ocular AO can only be achieved after these issues have been studied and understood. The cumulative research work over the last few years is beginning to provide enough data to improve our understanding of some of these issues.

#2904 - $15.00 US
Received August 15, 2003; Revised September 29, 2003

The dynamics of ocular aberrations is an area in which we posses very little information. Technological limitations and scarceness of data has made it a difficult problem to study. The little information available may be responsible for the general feeling within the adaptive optics community that the these dynamics do not occur at temporal frequencies above a few hertz and that attempt to correct high frequency fluctuations would not render a significant benefit. This has lead to the development of ocular adaptive optics systems with low frame rates. However, the results presented in this paper have shown that ocular aberrations can present dynamic behaviour faster than 30 Hz (Fig. 2) and that adaptive optics systems may benefit from faster correction.

It is evident from this and previous work that most of the degradation of image quality is produced by the lower frequency components of the aberrations. However, by increasing the speed of correction it seems to be possible to further improve the wavefront correction. This may be of greater importance as the technology currently available is not always able to match the amplitude of the slow changing variations while the relatively low amplitudes of the rapidly changing variations can be easily corrected. The dynamics of ocular aberrations are very likely to be partially responsible for the performance observed in our system.

The eye is part of a living system — constantly changing and adapting to its surroundings. Ocular movements, microsaccades, fluctuations in accommodation, changes in tear film thickness and intraocular pressure are all causes of aberration changes. Previous studies [9] have discarded ocular movements and microsaccades as possible sources of the large variability of ocular aberrations and have attributed it mainly to changes in tear film topography. Moreover, recent work by H. T. Kasprzak and J. W. Jaronski, [14] using an interferometric technique has shown evidence of changes in the ocular wavefront aberrations of up to 25 Hz. In their experiment, they observed the recorded interferogram to change form one frame to the next at video rate. Although their work does not provide an answer to the question of what the sources of the aberrations are, it is clear that these changes occur at least as fast as video rate — in agreement with our results. In addition, the power spectra we observed show the same slope as those reported by Hofer *et al.* [9], extending the same curve to frequencies up to 30 Hz.

The reader may note that the Strehl ratios in some subjects in Fig. 4 may appear low. This is very likely due to a limitation in the range of the deformable mirror. This same figure shows a large variability in bandwidth across and between subjects. This can be attributed to many causes: for an individual subject we can expect the dynamic behaviour of aberrations to be different for every run. It is very unlikely that every run will present exactly the same dynamic behaviour. For instance, we sometimes observed that as the subject became tired, the tear production increased, forcing us to stop the session for some time. Other physiological changes were more difficult to assess, such as breathing patterns, accommodative state, etc. producing a large uncertainty towards the source of this variability.

One plausible explanation for the variability between subjects may be in locating the Shack-

Table 1. Correlation and confidence values for the data in Fig. 4.

	Strehl Ratio vs Bandwidth			
Subject	**LD**	**JK**	**CT**	**CG**
Sample Size	7	11	19	19
Correlation (r)	0.558	0.612	0.427	0.422
Confidence (p)	0.192	0.045	0.068	0.071

#2904 - $15.00 US Received August 15, 2003; Revised September 29, 2003

Hartmann spots positions. A low signal to noise ratio (SNR) will increase the error in the position and hence reduce the system's bandwidth. We observed a subjective trend in this direction although it was not quantified. Further work in this direction is needed.

The aim of this research has been to study the impact of ocular aberration dynamics on the performance of an adaptive optics system. It has been shown that ocular adaptive optics systems may benefit from higher bandwidths. However, it is important to point out that correction bandwidth is only one of many factors that need to be studied and understood for optimising ocular adaptive optics. The bandwidth is used as a measure of the extent of temporal correction by the AO system as it is widely quoted by many authors. However, this single number does not describe the shape of the AO system's transfer function, and therefore has some limitations. For example, two different AO systems with the same bandwidth could give very different degrees of AO correction if one of them has a better suited system transfer function than the other.

We have left plenty of questions unanswered. There is neither a mechanism to explain the particular power spectrum observed, nor is there a statistical model describing or characterising these changes. The results of this work have shown the need of such models, not only to improve ocular adaptive optics, but also to improve our understanding of the visual system and how it interacts with its continuously changing surroundings. Ocular aberrations dynamics is also of vital importance for optimisation of surgical procedures for refractive surgery and other forms of static customised refractive correction. By understanding how and when ocular aberrations change, a better static correction may be achieved.

Acknowledgments

This research was supported in part by the European Union under contract number HPRN-CT-2002-00301 "SHARP-EYE".

#2904 - $15.00 US Received August 15, 2003; Revised September 29, 2003